β-Catenin destruction complex-independent regulation of Hippo–YAP signaling by APC in intestinal tumorigenesis

Jing Cai,[1,2] Anirban Maitra,[3] Robert A. Anders,[4] Makoto M. Taketo,[5] and Duojia Pan[1,2]

[1]Howard Hughes Medical Institute, [2]Department of Molecular Biology and Genetics, Johns Hopkins University School of Medicine, Baltimore, Maryland 21205, USA; [3]Sheikh Ahmed Bin Zayed Al Nahyan Center for Pancreatic Cancer Research, The University of Texas M.D. Anderson Cancer Center, Houston, Texas 77030; [4]Department of Pathology, Johns Hopkins University School of Medicine, Baltimore, Maryland 21205, USA; [5]Department of Pharmacology, Graduate School of Medicine, Kyoto University, Yoshida-Konoé-cho, Sakyo, Kyoto 606-8501, Japan

Mutations in *Adenomatous polyposis coli* (*APC*) underlie familial adenomatous polyposis (FAP), an inherited cancer syndrome characterized by the widespread development of colorectal polyps. APC is best known as a scaffold protein in the β-catenin destruction complex, whose activity is antagonized by canonical Wnt signaling. Whether other effector pathways mediate APC's tumor suppressor function is less clear. Here we report that activation of YAP, the downstream effector of the Hippo signaling pathway, is a general hallmark of tubular adenomas from FAP patients. We show that APC functions as a scaffold protein that facilitates the Hippo kinase cascade by interacting with Sav1 and Lats1. Consistent with the molecular link between APC and the Hippo signaling pathway, genetic analysis reveals that YAP is absolutely required for the development of *APC*-deficient adenomas. These findings establish Hippo–YAP signaling as a critical effector pathway downstream from APC, independent from its involvement in the β-catenin destruction complex.

[*Keywords*: β-catenin; APC; Hippo signaling; TAZ; YAP; tumorigenesis]

Supplemental material is available for this article.

Received April 24, 2015; revised version accepted June 19, 2015.

Adenomatous polyposis coli (APC) is the most commonly mutated tumor suppressor in human colorectal cancers (Markowitz and Bertagnolli 2009). APC is best known as a negative regulator of β-catenin, the downstream effector of canonical Wnt signaling (Gregorieff and Clevers 2005). In the absence of Wnt ligands, APC interacts with Axin2, casein kinase 1 (CK1), glycogen synthase kinase-3β (GSK-3β), and β-catenin in a destruction complex. This complex facilitates the sequential phosphorylation of β-catenin by CK1 and GSK-3β and its subsequent β-Trcp-mediated degradation. In the presence of Wnt ligands, the destruction complex is dissociated, which leads to stabilization of β-catenin and its nuclear accumulation. Besides its role in canonical Wnt signaling, APC has been reported to carry various cellular functions independent of β-catenin in regulating cytoskeleton, cell polarity, cell migration, and cell adhesion (Näthke 2006; Aoki and Taketo 2007). The extent to which such β-catenin-independent processes contribute to the tumor suppressor function of APC remains largely undefined. Understanding APC's β-catenin-dependent and β-catenin-independent tumor suppressor functions is important for the development of therapeutic approaches against *APC* mutant cancers (Lesko et al. 2014).

The Hippo signaling pathway is a conserved regulator of organ size in all animals (Pan 2010; Zhao et al. 2010a; Halder and Johnson 2011). In mammals, this pathway comprises a kinase cascade involving the Sav1/Mst kinase complex and the Mob1/Lats kinase complex that phosphorylates the transcription coactivators YAP and TAZ. Once phosphorylated, YAP and TAZ are sequestered in the cytoplasm and undergo β-Trcp-mediated degradation. Upon inactivation of the Hippo pathway, stabilized YAP and TAZ translocate into the nucleus to activate target gene transcription.

Corresponding author: djpan@jhmi.edu
Article published online ahead of print. Article and publication date are online at http://www.genesdev.org/cgi/doi/10.1101/gad.264515.115.

We showed previously that inactivation of the Hippo pathway tumor suppressor Sav1 in mouse intestines results in activation of the YAP oncoprotein and the development of sessile serrated polyps (SSPs) (Cai et al. 2010), which are precursors for less than one-third of human colorectal cancer (Rex et al. 2012). In contrast, YAP overexpression and/or nuclear accumulation were reported in the majority of 28 uncategorized human colon cancer samples in one study (Steinhardt et al. 2008) and in 68 out of 71 colon carcinomas in another study (Zhou et al. 2011). Such discrepancies suggest the existence of a more pervasive mechanism that restricts YAP activity in normal intestinal epithelia. Since APC is mutated in nearly all human colorectal cancers (Markowitz and Bertagnolli 2009), an attractive hypothesis is that loss of APC may be the underlying cause for the prevalent activation of YAP observed in these cancers.

In this study, we used a combination of in vivo mouse genetics and in vitro cell culture analysis to investigate the relationship between APC and YAP in intestinal tumorigenesis. In contrast to a recent study suggesting that APC directly regulates the degradation of YAP/TAZ through the β-catenin destruction complex (Azzolin et al. 2014), we report a distinct mechanism by which APC negatively regulates YAP activity. This mechanism is mediated not by the β-catenin destruction complex but rather a novel function of APC as a scaffold protein that facilitates the phosphorylation of YAP/TAZ through the Hippo kinase cascade. Our studies support the view that APC dually regulates YAP and β-catenin through parallel pathways involving the Hippo kinase cascade and the destruction complex, respectively.

Results

Activation of YAP in APC*-deficient mouse intestinal adenomas, human tubular adenomas, and acinar cell carcinomas*

The coprevalence of YAP activation and *APC* mutations in human colorectal cancers prompted us to investigate whether APC deficiency may lead to YAP activation. To test this hypothesis, we first took advantage of the well-characterized mouse model APC^{Min}/+, in which somatic inactivation of the wild-type *APC* allele results in widespread adenomas throughout the gastrointestinal tract (Moser et al. 1990; Su et al. 1992). The neoplastic epithelia showed not only the expected nuclear accumulation of β-catenin (Fig. 1A) but also nuclear accumulation and overall increase of YAP (Fig. 1B). Despite the increase in YAP staining, the neoplastic epithelia showed similar staining intensity of phospho-YAP^{S112} compared with the neighboring nonneoplastic epithelia (Fig. 1C), suggesting that the relative YAP phosphorylation might be compromised in the APC^{Min}/+ neoplastic epithelia. To investigate this more quantitatively, we analyzed cell lysates of normal and adenoma tissues from the APC^{Min}/+ colons by Western blotting. Consistent with immunohistochemical

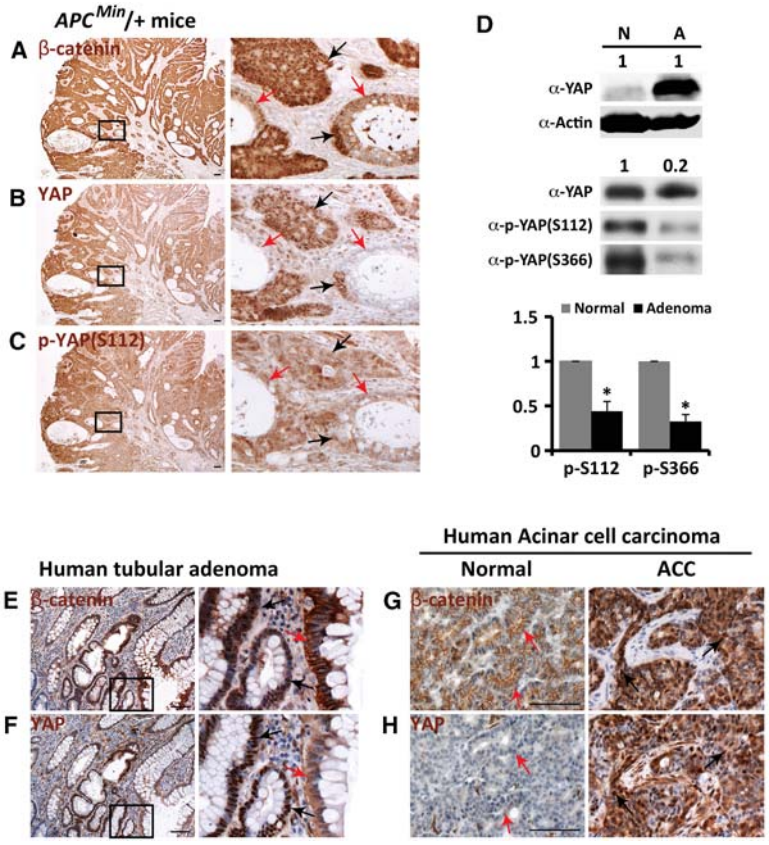

Figure 1. YAP activation in APC^{Min}/+ mouse colonic adenomas, human tubular adenomas, and acinar cell carcinomas. (*A–C*) β-Catenin, YAP, and p-YAP staining in serial sections of 3-mo-old APC^{Min}/+ mouse colonic adenomas. Black arrows indicate neoplastic colonic epithelia, and red arrows indicate their nonneoplastic neighbors. Bar, 100 µm. (*D*) Western blot analysis. Protein extracts from normal tissues (N) and adenomas (A) of 3-mo-old APC^{Min}/+ mouse colons were probed with the indicated antibodies. (*Top* gels) Equal amounts of normal and adenoma extracts were analyzed (1:1). (*Bottom* gels) Normal extract and fivefold less adenoma extract (1:0.2) were analyzed for YAP, p-YAP^{S112}, and p-YAP^{S366}. The ratios of p-YAP^{S112} over total YAP and of p-YAP^{S366} over total YAP were quantified. Data are mean ± SD. $n = 3$. (*) $P < 0.001$, *t*-test. (*E,F*) β-Catenin and YAP staining in serial sections of human tubular adenomas. Black arrows indicate neoplastic colonic epithelia, and red arrows indicate their nonneoplastic neighbors. Bar, 100 µm. (*G,H*) β-Catenin and YAP staining in serial sections of human acinar cell carcinomas (ACCs). Black arrows indicate acinar cell carcinomas, and red arrows indicate normal acinar cells. Bar, 100 µm.

staining, adenoma lysates contained much higher levels of total YAP than the normal lysates (Fig. 1D). This increase was not simply due to the expansion of colonic crypts, which are known to be YAP-positive (Cai et al. 2010), in the adenoma, since, when YAP loading was adjusted to comparable levels, it was evident that phosphorylation of YAP at both S112 and S366 (corresponding to S127 and S381 of human YAP) was significantly decreased in the APC^{Min}/+ adenomas compared with the nonneoplastic tissues from the same animal (Fig. 1D).

The nuclear accumulation and overall increase of YAP in APC^{Min}/+ adenomas prompted us to investigate whether YAP is also activated in tubular adenomas of familial adenomatous polyposis (FAP) patients, who carry germline mutations in one allele of *APC* and develop hundreds of adenomas in the colon after inactivation of the wild-type allele by loss of heterozygosity. We therefore examined YAP and β-catenin staining in an archival collection of 175 histologically documented tubular adenomas that had been endoscopically removed from FAP patients. As expected, the majority of the adenomas (149 out of 175) showed nuclear accumulation of β-catenin (Fig. 1E; Supplemental Fig. S1). Strikingly, nearly all of the adenomas (174 out of 175) exhibited nuclear accumulation of YAP in the neoplastic epithelia compared with their nonneoplastic neighbors (Fig. 1F; Supplemental Fig. S1), suggesting that YAP activation is a general hallmark of tubular adenomas. Besides tubular adenomas, mutations in *APC* are also frequently detected in human pancreatic acinar cell carcinomas (Abraham et al. 2002). Examination of an archival collection of 43 histologically documented pancreatic acinar cell carcinomas revealed that the majority of them showed nuclear accumulation of β-catenin (37 out of 43) and YAP (38 out of 43) (Fig. 1G,H; Supplemental Fig. S1). Thus, YAP activation is observed in multiple *APC*-deficient tumor types in mice and humans.

YAP is activated by acute loss of APC but not by activation of β-catenin

To demonstrate that YAP activation is a direct consequence of APC deficiency rather than a secondary consequence of adenoma formation, we generated *Lgr5-EGFP-IRES-creER*^{T2};$APC^{flox/flox}$ mice. Intraperitoneal injection of tamoxifen induced acute loss of APC in a fraction of intestinal stem cells as described (Barker et al. 2009). Fifteen days after tamoxifen injection, nuclear accumulation of β-catenin, an indication of APC inactivation, was observed in the jejunal crypts in a mosaic pattern (Fig. 2A). Like the APC^{Min}/+ adenomas, the crypts with acute APC inactivation also showed much higher YAP staining than the neighboring nonmutant crypts (Fig. 2B), while phospho-YAP^{S112} staining intensity was comparable between the two types of crypts (Fig. 2C). These results suggest that acute loss of APC also activates YAP.

It was reported that β-catenin can promote the mRNA expression or protein stability of YAP (Konsavage et al. 2012; Wang et al. 2013). These findings raise the possibility that YAP activation after loss of APC may be merely due to increased β-catenin activity. To examine this possibility, we used the same *Lgr5-EGFP-IRES-creER*^{T2} driver described above to express a stabilized and activated form of β-catenin (Δex3) (Harada et al. 1999). Fifteen days after tamoxifen injection in the *Lgr5-EGFP-IRES-creER*^{T2};$Catnb^{+/lox(ex3)}$ mice, stabilized nuclear β-catenin was expressed in the jejunal crypts in a mosaic pattern (Fig. 2D). Despite the activation of β-catenin in both *Lgr5-EGFP-IRES-creER*^{T2}-induced models, the *APC*-deficient and β-catenin-stabilized models differ in the status of YAP. Unlike the nuclear accumulation of YAP in the *APC*-deficient crypts (Fig. 2B), the β-catenin-stabilized crypts showed diffuse YAP staining throughout the cell without clear nuclear accumulation (Fig. 2E). Meanwhile, the β-catenin-stabilized crypts showed slightly increased phospho-YAP^{S112} staining compared with the normal epithelia (Fig. 2F). We inferred from these observations that Hippo signaling activity, as indicated by the relative ratio of phospho-YAP^{S112} versus total YAP, was decreased in the *APC*-deficient crypts but not the β-catenin-stabilized crypts. This was confirmed by Western blot analysis of cell lysates from *APC*-deficient and β-catenin-stabilized jejunal tissues. While lysates from both mutant tissues showed increased YAP protein levels, the relative p-YAP^{S112}/YAP or p-YAP^{S366}/YAP ratios were decreased only in the *APC*-deficient tissues (Fig. 2G). Thus, loss of APC, but not activation of β-catenin, impairs YAP phosphorylation and activates YAP.

APC functions as a scaffold protein that facilitates the Hippo kinase cascade

The effect of APC inactivation on YAP phosphorylation in the intestines resembles that caused by loss of Sav1 or Mst1/2 (Cai et al. 2010; Zhou et al. 2011), suggesting that APC may regulate YAP phosphorylation through the Hippo pathway. To investigate this further, we analyzed the status of Mst1/2 and Lats1/2 phosphorylation in jejunal lysates from the *Lgr5-EGFP-IRES-creER*^{T2};$APC^{flox/flox}$ mice. Like YAP, the Lats1 protein level was dramatically increased in the *APC*-deficient jejunum. This is at least partly due to the expansion of jejunal crypts, which normally express much higher levels of Lats1 (Supplemental Fig. S2). When Lats1 loading was adjusted to comparable levels, it was evident that the relative ratio of phosphorylated Lats to total Lats1 (p-Lats/Lats1), but not p-Mst/Mst1, was decreased in *APC*-deficient tissues (Fig. 2H). These results suggest that APC intersects the Hippo kinase cascade upstream of Lats1 activation.

To complement the genetic analysis, we examined the effect of APC on the Hippo kinase cascade in cultured cells. Consistent with our in vivo observations, RNAi knockdown of *APC* in HEK293 cells resulted in decreased phosphorylation of YAP and Lats1/2 but not Mst1/2 (Fig. 2I). The effect of APC RNAi on YAP phosphorylation resembles that of Lats1/2 RNAi (Fig. 2I). We further confirmed this result by engineering APC-null HEK293 cells using the CRISPR/Cas9 technology. Compared with the parental HEK293 cells, APC-null HEK293 cells showed decreased phosphorylation of YAP and Lats1/2 without affecting Mst1/2 phosphorylation (Fig. 2I). We note that loss

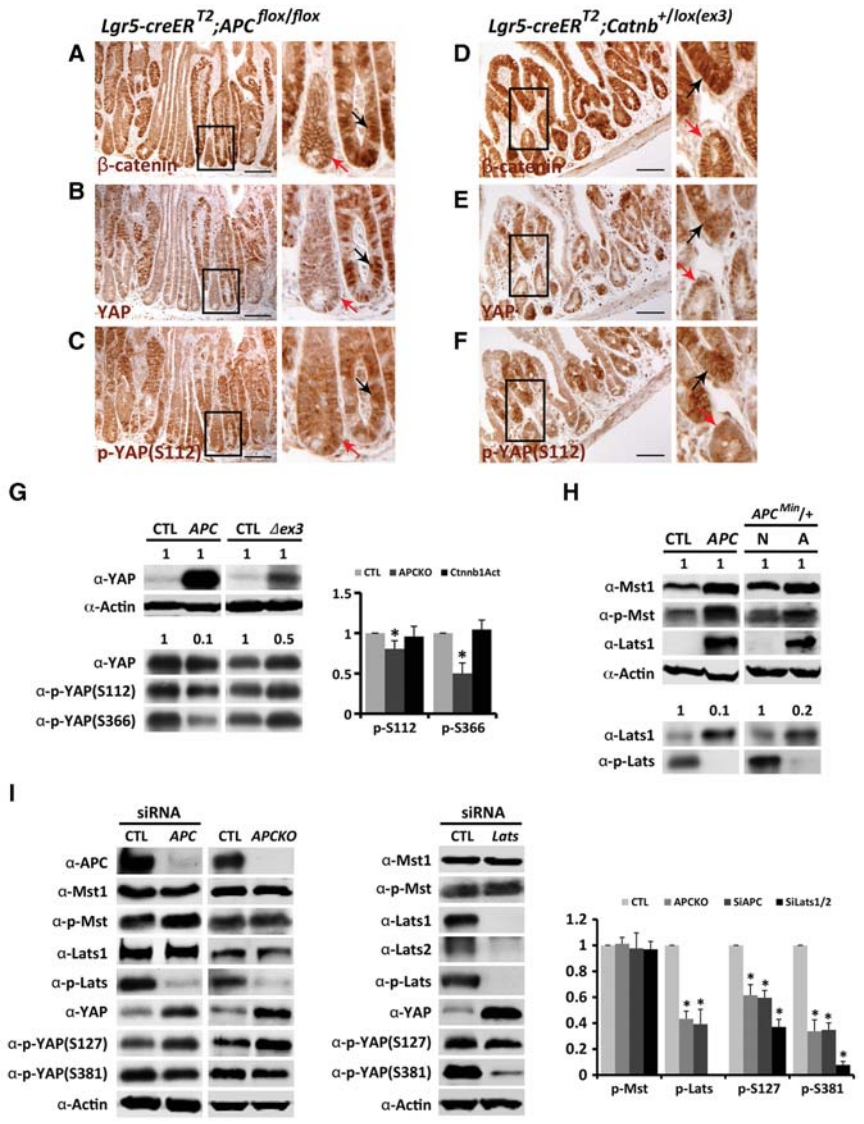

Figure 2. APC functions independently of β-catenin to restrict YAP activity. (*A–C*) β-Catenin, YAP, and p-YAP staining in serial sections of *APC*-deficient (*Lgr5-EGFP-IRES-creER*^{T2}*;APC*$^{flox/flox}$) jejunum 15 d after tamoxifen injection. Black arrows indicate *APC*-deficient crypts, and red arrows indicate normal crypts. Bar, 100 µm. (*D–F*) β-Catenin, YAP, and p-YAP staining in serial sections of β-catenin-stabilized (*Lgr5-EGFP-IRES-creER*^{T2}*;Catnb*$^{+/lox(ex3)}$) jejunum 15 d after tamoxifen injection. Black arrows indicate β-catenin-stabilized crypts, and red arrows indicate normal crypts. Bar, 100 µm. (*G*) Western blot analysis. Protein extracts from *APC*-deficient, β-catenin-stabilized, and control jejunal tissues 4 wk after tamoxifen injection were probed with the indicated antibodies. (*Top* gels) Equal amounts of the indicated extracts (1:1) were analyzed. (*Bottom* gels) Normal and diluted mutant extracts (1:0.1 for *APC*, and 1:0.5 for Δex3) were analyzed for YAP, p-YAP^{S112}, and p-YAP^{S366}. The ratios of p-YAP^{S112} over total YAP and of p-YAP^{S366} over total YAP were quantified. Data are mean ± SD. $n = 3$. (*) $P < 0.05$, *t*-test. (*H*) Western blot analysis. Protein extracts from *APC*-deficient and control jejunal tissues 4 wk after tamoxifen injection and protein extracts from normal tissues and adenomas of 3-mo-old *APC*^{Min}/+ mouse colons were probed with the indicated antibodies. (*Top* gels) Equal amounts of the indicated extracts (1:1) were analyzed. (*Bottom* gels) Normal and diluted mutant extracts (1:0.1 for *APC* mutant, and 1:0.2 for *APC*^{Min}/+ adenoma) were analyzed for Lats1 and p-Lats. (*I*) Western blot analysis. Protein extracts from HEK293 (control), HEK293 with CRISPR–Cas9-engineered *APC* knockout (*APCKO*), and HEK293 cells with *APC* or *Lats1/2* RNAi were probed with the indicated antibodies. The ratios of p-Mst over Mst1, p-Lats over Lats1, p-YAP^{S112} over total YAP, and p-YAP^{S366} over total YAP were quantified. Data are mean ± SD. $n = 3$. (*) $P < 0.001$, *t*-test.

of APC in HEK293 cells by either RNAi or CRISPR/Cas9 knockout did not affect Lats1 protein level, which supports our view that the dramatic increase of Lats1 in the *APC*-deficient jejunal lysates is not due to the stabilization of Lats1 per se but rather the expansion of the Lats1-positive crypts (Supplemental Fig. S2). Taken together, both in vivo and in vitro analyses implicate APC as a regulator of the Hippo kinase cascade acting upstream of Lats1 activation.

To investigate how APC intersects the Hippo pathway, we examined potential interactions between APC and core components of the Hippo kinase cascade. Coimmunoprecipitation (co-IP) assays with epitope-tagged proteins revealed that APC interacted with Sav1 and Lats1 (Fig. 3A,B) but not Mst2, Mob1, or YAP in HEK293 cells (Supplemental Fig. S3A–C). These interactions were confirmed between endogenous APC and Lats1 and between endogenous APC and HA-tagged Sav1 (Fig. 3C). Interestingly, previous studies of Hippo pathway interactome using immunoprecipitation–mass spectrometry have identified APC as a Hippo pathway-interacting protein in both *Drosophila* and mammalian cells: APC was identified in HeLa cells in Lats2 immunoprecipitation (Couzens et al. 2013) and in *Drosophila* S2R^{+} cells in the immunoprecipitation of multiple Hippo pathway core components, including Hpo, Sav, Wts, and Yki (Kwon et al. 2013). These results suggest that APC, through its conserved interactions with Sav1 and Lats, may serve as a scaffold that facilitates the formation of the Hippo core kinase cassette and hence promotes Lats activation. Consistent with this hypothesis, overexpression of APC specifically enhanced Sav1–Lats1interactions (Fig. 3D) without affecting Mst2–Sav1 or Lats1–Mob1 interactions in HEK293 cells (Supplemental Fig. S3D,E). Conversely,

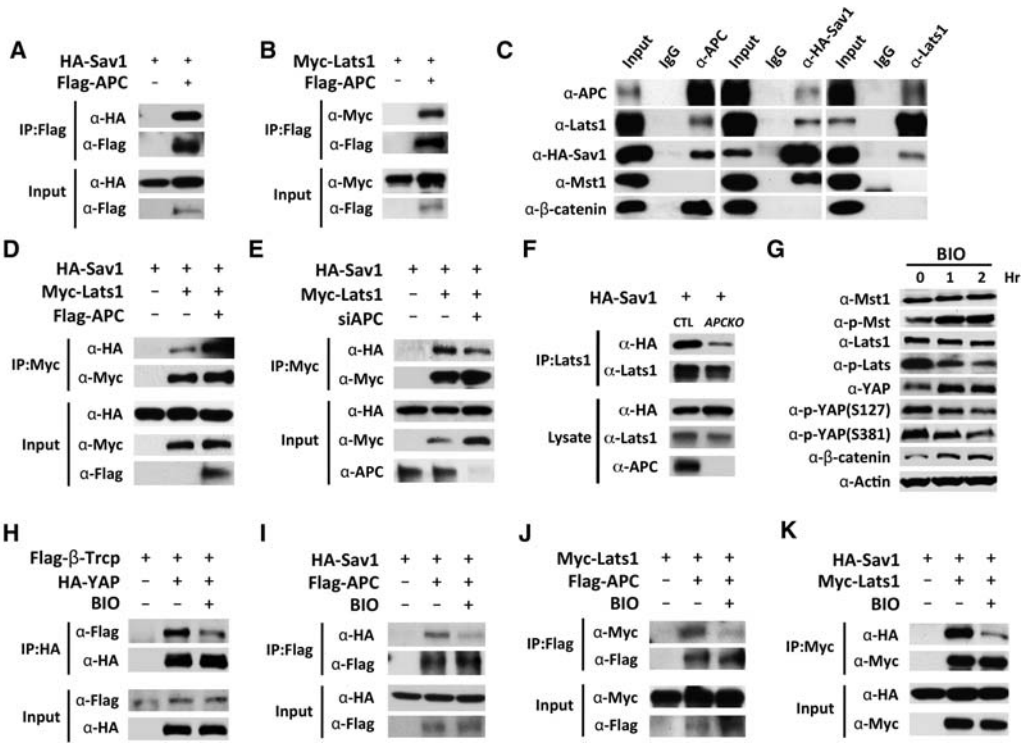

Figure 3. Physical interactions among APC, Sav1, and Lats1 and their regulation by GSK-3β. (*A–C*) APC interacts with Sav1 and Lats1 in HEK293 cells. (*A*,*B*) Co-IP between Flag-APC and HA-Sav1 or Myc-Lats1. (*C*) Co-IP between endogenous APC and Lats1 and between endogenous APC and HA-Sav1. HA-Sav1 was used for co-IP analysis because endogenous Sav1 expression is very low in HEK293 cells. (*D*) Overexpression of APC enhanced Sav1–Lats1 interactions. (*E*) siRNA knockdown of endogenous *APC* decreased Sav1–Lats1 interactions. (*F*) HEK293 (control) and HEK293 with CRISPR–Cas9-engineered *APC* knockout (*APCKO*) were analyzed for co-IP between Sav1 and endogenous Lats1, showing reduced Sav1–Lats1 interaction in the APC knockout cells. (*G*) Western blot analysis of HEK293 cells after 6-bromoindirubin-3′-oxime (BIO) treatment for the indicated times. (*H*) Co-IP analysis of β-Trcp–YAP interactions. Note the reduction of β-Trcp–YAP interactions in HEK293 cells treated with BIO for 1 h. (*I–K*) similar to *H* except that APC–Sav1 (*I*), APC–Lats1 (*J*), and Sav1–Lats1 (*K*) interactions were analyzed.

both RNAi knockdown and CRISPR/Cas9-mediated knockout of endogenous APC impaired Sav1–Lats1 interactions in HEK293 cells (Fig. 3E,F).

The scaffolding function of APC in facilitating the Hippo kinase cascade is regulated by GSK-3β but not Wnt3a

The results presented above suggest that APC directly regulates the Hippo kinase cascade independently of the Wnt signaling effector β-catenin. To investigate whether the scaffolding function of APC in the Hippo kinase cascade is regulated, we first examined the effect of Wnt3a, a ligand for canonical Wnt signaling. Treating HEK293 cells with recombined human Wnt3a resulted in β-catenin accumulation but had no effect on Mst, Lats, or YAP phosphorylation (Supplemental Fig. S3F). Likewise, stabilization of Axin2 by XAV939, a tankyrase inhibitor, had no effect on Lats or YAP phosphorylation (Supplemental Fig. S3G). In contrast, inhibition of GSK-3β activity with 6-bromoindirubin-3′-oxime (BIO) resulted in not only β-catenin accumulation but also decreased phosphorylation of Lats and YAP (at both YAP^{S127} and YAP^{S381}) as well as increased YAP protein levels (Fig. 3G). Consistent with a previous report that YAP^{S381} phosphorylation leads to β-Trcp-mediated YAP degradation (Zhao et al. 2010b), BIO treatment reduced the interactions between YAP and β-Trcp (Fig. 3H), which likely accounts for BIO-induced accumulation of endogenous YAP in HEK293 cells (Fig. 3G). Further analysis revealed that BIO treatment reduced the physical interactions among APC, Sav1, and Lats1 (Fig. 3I–K) but not Mst2–Sav1 or Lats1–Mob1 interactions (Supplemental Fig. S3H,I). These results suggest that the scaffold function of APC in facilitating the Hippo kinase cascade is regulated by GSK-3β, although the direct substrate of GSK-3β in this regulation remains to be determined. Taken together, we suggest that APC and GSK-3β are common regulators of two parallel pathways: Wnt–β-catenin and Hippo–YAP signaling.

YAP/TAZ and β-catenin are not coregulated by a shared destruction complex in HEK293 cells or mouse intestines

Our findings that loss of APC activates YAP due to impaired Hippo kinase cascade differ from a recent report

suggesting that YAP/TAZ and β-catenin are coregulated by canonical Wnt signaling through the same APC-containing destruction complex (Azzolin et al. 2014). According to this model, canonical Wnt signaling or loss of APC would disengage the destruction complex, thereby stabilizing YAP/TAZ and β-catenin directly. However, we found that Wnt3a did not stimulate a YAP-TEAD reporter (8xGTIIC-Lux) in HEK293 cells even though it stimulated a Wnt signaling reporter (TOP-FLASH) under the same conditions (Supplemental Fig. S4A,B). Using a validated YAP-specific antibody (Novus Biologicals, NB110-58358), we found that Wnt3a did not induce YAP nuclear localization in HEK293 cells despite inducing β-catenin stabilization (Supplemental Figs. S4C,D, S5). These findings suggest that, at least in HEK293 cells, the Wnt-regulated β-catenin destruction complex does not regulate YAP activity.

Based on studies in cultured cells, it was suggested that both YAP/TAZ and β-catenin are mutually required for the assembly of the destruction complex (Azzolin et al. 2012, 2014). According to this model, loss of β-catenin should result in activation of YAP/TAZ, and, conversely, loss of YAP/TAZ should result in activation of β-catenin. We tested this prediction genetically in mouse intestines. We observed no changes in YAP/TAZ abundance or subcellular localization in β-*catenin*-deficient colonic epithelium (Supplemental Fig. S4E), and, conversely, β-catenin abundance or subcellular localization was not altered in colonic epithelium after loss of YAP and TAZ (Supplemental Fig. S4F). Thus, at least in the intestines, YAP/TAZ and β-catenin are not codependent on each other for degradation. These observations are consistent with previous analysis of SSPs in human and *Sav1*-deficient mouse colons, which exhibit nuclear accumulation of YAP without activation of β-catenin (Cai et al. 2010), and are also consistent with the uncoupled regulation of YAP and β-catenin in ovarian serous carcinomas or pancreatic ductal adenocarcinomas, which rarely have *APC* mutations (Supplemental Fig. S1).

It is worth noting that the *APC*-deficient intestinal epithelia or adenomas showed not only nuclear accumulation of YAP but also decreased YAP and Lats phosphorylation. These phenotypes are indicative of Hippo signaling defects and cannot be readily explained by direct regulation of YAP through the β-catenin destruction complex. Thus, although YAP and β-catenin may be coregulated by the same destruction complex in some cellular contexts, our findings do not support this coregulation in the intestines.

The combined activation of YAP and β-catenin contributes to the APC*-deficient intestinal phenotypes*

The above results, together with its well-established role in Wnt signaling, implicate APC as a dual regulator of both Wnt–β-catenin and Hippo–YAP signaling. We conducted further genetic analysis to corroborate this model. A straightforward prediction of our model is that the combined activation of YAP and β-catenin should more closely resemble loss of APC than the activation of each single effector. We tested this prediction by combining loss of Sav1, a well-characterized negative regulator of YAP, with the activated β-catenin mutant β-catenin$^{\Delta ex3}$.

We used the *Lgr5-EGFP-IRES-creER*^{T2} driver described above to achieve tamoxifen-induced loss of Sav1, expression of stabilized β-catenin mutant Δex3, or loss of APC in adult mice (Fig. 4). All analyses were conducted 4 wk after tamoxifen injection. Normal jejunum shows clear crypt–villus transition, with Ki67-positive cells restricted to the crypt at the bottom of the crypt–villus axis. Tamoxifen-induced loss of Sav1 did not produce any overt phenotype in the jejunum by histological analysis or Ki67 staining. Tamoxifen-induced loss of APC resulted in greatly expanded, tubular-shaped crypts with Ki67 staining spanning the whole crypt–villus axis, while tamoxifen-induced expression of β-catenin$^{\Delta ex3}$ resulted in a milder phenotype with less expansion of the crypt structures and Ki67 staining. Interestingly, when combined with β-catenin$^{\Delta ex3}$, loss of Sav1 greatly enhanced the mutant phenotype of β-catenin$^{\Delta ex3}$. Histologically, the double-mutant jejunum no longer showed distinct crypt–villus transition, since the crypt structures and Ki67 staining were greatly expanded to cover the whole crypt–villus axis (Fig. 4A,B). Furthermore, unlike the β-catenin$^{\Delta ex3}$ jejunum, which showed diffuse YAP staining throughout the cell without clear nuclear accumulation, the β-*catenin*$^{\Delta ex3}$;*Sav1* double-mutant jejunum showed prominent nuclear accumulation of YAP (Fig. 4C). β-*catenin*$^{\Delta ex3}$;*Sav1* double-mutant jejunum also grew polyps with adenomatous transformation, which was more severe than activation of β-catenin only and more closely resembled the polyps in the *APC*-deficient jejunum (Supplemental Fig. S6). These double-mutant phenotypes more closely resemble those resulting from loss of APC (Fig. 4A–C; Supplemental Fig. S6), supporting the view that activation of both YAP and β-catenin contributes to the *APC*-deficient phenotypes.

The phenotypic analysis presented above was further supported by microarray analysis of gene expression profiling of the various mutant backgrounds. We identified 1272 genes that were up-regulated in the β-*catenin*$^{\Delta ex3}$;*Sav1* double-mutant jejunum compared with the β-*catenin*$^{\Delta ex3}$ jejunum and 2641 genes that were up-regulated in the *APC* mutant jejunum compared with the β-*catenin*$^{\Delta ex3}$ jejunum (Fig. 4D). The former genes likely represent genes that are selectively responsive to YAP, while the latter genes represent β-catenin-independent targets of APC. Significantly, 990 genes are shared between the two gene sets (Fig. 4D). Furthermore, these shared genes generally showed similar levels of expression in the β-*catenin*$^{\Delta ex3}$;*Sav1* double-mutant and the *APC* mutant jejunum (Fig. 4E; Supplemental Table S1). These data support the view that YAP activation represents a significant portion of the β-catenin-independent output downstream from APC. Gene set enrichment analysis revealed that these YAP-dependent, β-catenin-independent APC targets are enriched for genes involved in growth, cell proliferation, and immune response (Fig. 4F).

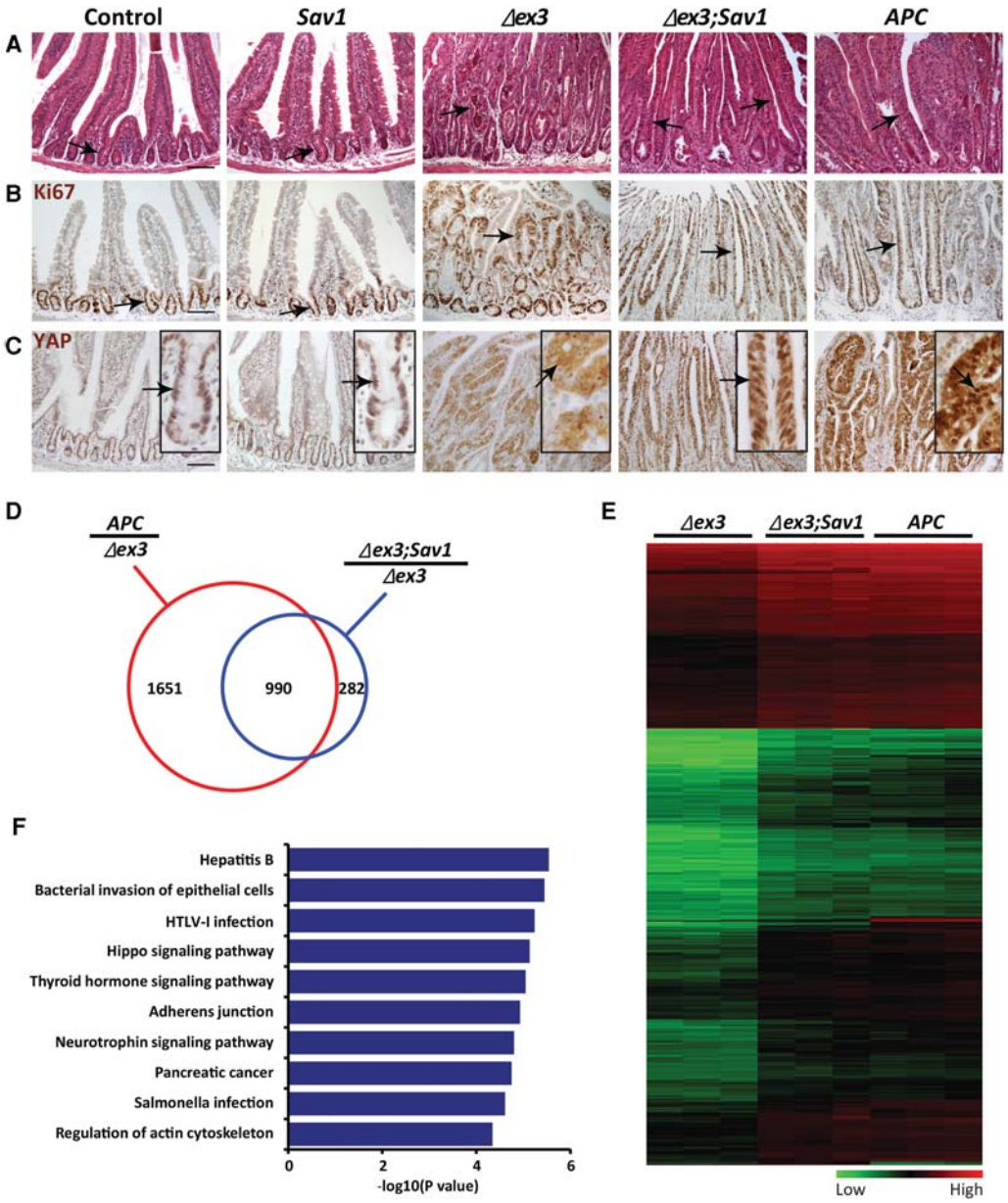

Figure 4. The combined activation of YAP and β-catenin resembles the *APC*-deficient phenotype. (*A–C*) Histology (*A*), Ki67 staining (*B*), and YAP staining (*C*) in control, *Sav1* mutant (*Lgr5-EGFP-IRES-creER*^{T2};*Sav1*$^{flox/flox}$), β-*catenin*$^{\Delta ex3}$ (*Lgr5-EGFP-IRES-creER*^{T2};*Catnb*$^{+/lox(ex3)}$), β-*catenin*$^{\Delta ex3}$;*Sav1* double-mutant (*Lgr5-EGFP-IRES-creER*^{T2};*Catnb*$^{+/lox(ex3)}$;*Sav1*$^{flox/flox}$), and *APC* mutant (*Lgr5-EGFP-IRES-creER*^{T2};*APC*$^{flox/flox}$) jejunum 4 wk after tamoxifen injection. Black arrows indicate crypts. Bar, 100 µm. (*D*) Microarray analysis. The red circle indicates genes up-regulated by at least twofold in *APC* mutant jejunum compared with β-*catenin*$^{\Delta ex3}$ jejunum. The blue circle indicates genes up-regulated by at least twofold in β-*catenin*$^{\Delta ex3}$;*Sav1* double-mutant jejunum compared with β-*catenin*$^{\Delta ex3}$ jejunum. Nine-hundred-ninety genes representing the overlap of the two gene sets are also shown. (*E*) Heat map analysis of expression profiles of the 990 shared genes that represent YAP-dependent, β-catenin-independent targets downstream from APC. (*F*) The top 10 enriched pathways as detected by gene set enrichment analysis of the 990 genes. The 990 shared genes that represent YAP-dependent, β-catenin-independent targets downstream from APC were analyzed.

YAP is functionally required for intestinal tumorigenesis resulting from loss of APC

To assess the physiological relevance of YAP as a downstream effector of the APC tumor suppressor, we examined whether inactivation of YAP could suppress adenoma formation in the *APC*^{Min}/+ mice. We showed previously that YAP is dispensable in normal intestinal development and homeostasis, as *VilCre;Yap*$^{flox/flox}$ mice are morphologically indistinguishable from wild-type control mice (Cai et al. 2010). On the other hand, the *APC*^{Min}/+ mice develop widespread adenomas throughout the gastrointestinal tract (Moser et al. 1990; Su et al. 1992). Strikingly, introducing loss of YAP into the *APC*^{Min}/+ model (*VilCre;APC*^{Min}/+;

Yap$^{flox/flox}$) nearly completely abolished adenoma formation in both the small intestine and the colon (Fig. 5A). The rare adenomas remaining in these animals were due to escaper cells that did not express Cre (as revealed by negative *Rosa26LacZ* reporter activity in the neoplastic epithelia) (Fig. 5B) and therefore failed to delete the *Yap* gene (as revealed by positive YAP staining and the presence of *Yap* mRNA in the neoplastic epithelia) (Fig. 5C,D). Consistent with the reduction in tumor burden, the life span of the *VilCre;APC*^{Min}/+;*Yap*$^{flox/flox}$ mice was significantly prolonged compared with the *APC*^{Min}/+ mice (Fig. 5E).

We further extended our analysis of YAP requirement to another intestinal adenoma model, *VilCre;APC*^{flox}/+, in which APC is inactivated by Cre-mediated excision of the *APC*^{flox} allele and loss of the remaining wild-type allele. This model develops multiple adenomas in the small intestine and rare adenomas in the colon (less than one colon adenoma per animal) (Supplemental Fig. S7A). A complete suppression of adenoma formation in the small intestines of *VilCre;APC*^{flox}/+;*Yap*$^{flox/flox}$ mice was observed compared with *VilCre;APC*^{flox}/+ mice (Supplemental Fig. S7A). The remaining adenomas in the colons of *VilCre;APC*^{flox}/+;*Yap*$^{flox/flox}$ mice were all positive for YAP staining (Supplemental Fig. S7B,C), suggesting that they were derived from *APC*$^{-/-}$ cells that had escaped *Yap* deletion. Taken together, our findings that loss of YAP abolishes adenoma formation in two different models of *APC*-deficient adenomas (*APC*^{Min}/+ and *VilCre;APC*^{flox}/+) demonstrate that YAP is functionally required for the development of *APC*-deficient adenomas. Thus, inasmuch as YAP is activated by loss of canonical Hippo pathway tumor suppressors such as Sav1 or Mst1/2 and is required for the development of *Sav1*- or *Mst1/2*-deficient adenomas (Cai et al. 2010; Zhou et al. 2011), YAP is also activated by loss of the APC tumor suppressor and is required for *APC*-deficient adenomas.

TAZ is transcriptionally regulated by YAP and β-catenin and is functionally required for intestinal tumorigenesis resulting from loss of APC

YAP and its paralog, TAZ, are generally believed to be regulated similarly by the Hippo pathway through phosphorylation-dependent degradation. Indeed, constitutive loss of Sav1 in the *VilCre;Sav1*$^{flox/flox}$ intestines resulted in increased YAP protein levels (Cai et al. 2010). However, the effect of Sav1 inactivation on TAZ had not been analyzed before. We found that TAZ protein levels were also increased upon constitutive loss of Sav1 in these animals (Fig. 6A). Unexpectedly, *Taz* mRNA levels were

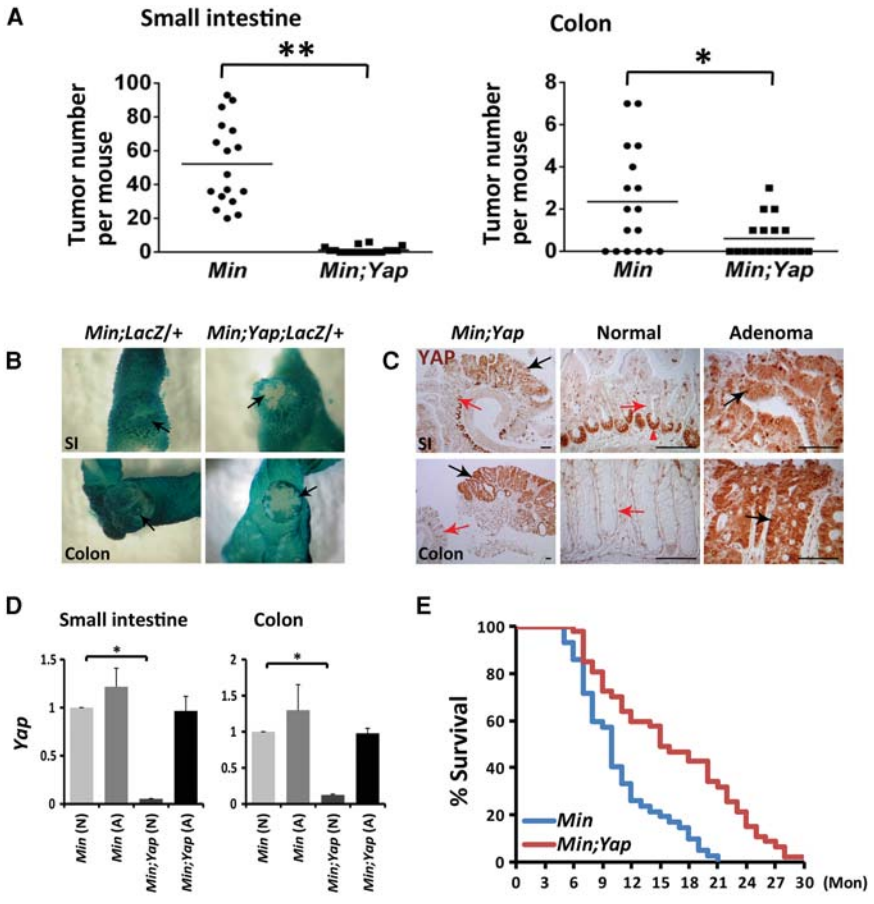

Figure 5. YAP is required for intestinal tumorigenesis in *APC*^{Min}/+ mice. (*A*) Quantification of the number of adenomas in the small intestines and the colons of 17 *APC*^{Min}/+;*Yap*$^{flox/flox}$ (*Min*) and 18 *VilCre;APC*^{Min}/+;*Yap*$^{flox/flox}$ (*Min;Yap*) mice at the age of 3 mo. (*) $P < 0.005$; (**) $P < 0.001$, *t*-test. (*B*) β-Galactosidase staining of *Rosa26LacZ* reporter in *VilCre;APC*^{Min}/+;*Rosa26LacZ*/+ (*Min;LacZ*/+) and *VilCre;APC*^{Min}/+;*Yap*$^{flox/flox}$;*Rosa26LacZ*/+ (*Min;Yap;LacZ*/+) intestines. Note the blue (*LacZ*-positive) adenomas in the small intestines (SI) and colons of control *Min;LacZ*/+ mice and the white (*LacZ*-negative) adenomas in the colon and small intestine of *Min;Yap;LacZ*/+ mice. Black arrows indicate adenomas. (*C*) YAP staining in the rare adenomas in the small intestines (SI) and colons of *Min;Yap* mice. Note the absence of YAP staining in the nonneoplastic crypts (red arrows) and positive YAP staining in the neoplastic epithelia (black arrows). The red arrowhead indicates nonspecific staining of the antibody in the paneth cells in the ilea. Bar, 100 µm. (*D*) Real-time PCR analysis of *Yap* mRNA levels in normal tissues (N) and adenomas (A) from the small intestines and colons of *APC*^{Min}/+;*Yap*$^{flox/flox}$(*Min*) and *VilCre;APC*^{Min}/+;*Yap*$^{flox/flox}$ (*Min;Yap*) mice. Note the sustained expression of *Yap* in *Min;Yap* adenomas but not *Min;Yap* normal tissues. Data are mean ± SD. $n = 3$. (*) $P < 0.005$, *t*-test. (*E*) Significantly prolonged life span in the *Min;Yap* mice compared with the control *Min* mice. Forty-two *APC*^{Min}/+;*Yap*$^{flox/flox}$ (*Min*) and 47 *VilCre;APC*^{Min}/+;*Yap*$^{flox/flox}$ (*Min;Yap*) mice were used for analysis. (Mon) Months.

dramatically up-regulated (>40-fold) in the *Sav1*-deficient crypts (Fig. 6B), and this up-regulation was completely reversed in *Sav1;Yap* double-mutant crypts (Fig. 6B). These results suggest that TAZ is regulated not only post-transcriptionally through Hippo-mediated phosphorylation but also transcriptionally through YAP. However, unlike YAP, whose inactivation completely suppressed the enlarged and hyperplastic crypt phenotypes in *Sav1*-deficient intestines (Cai et al. 2010), loss of TAZ failed to suppress these *Sav1*-deficient phenotypes (Fig. 6C), suggesting that YAP is a more essential effector downstream from the Hippo pathway in the intestine.

Interestingly, we found that both TAZ protein and *Taz* mRNA levels were also up-regulated in *APC* or β-*catenin*$^{\Delta ex3}$ jejunum (Fig. 6D,E). While the increase in *Taz* mRNA levels in the *APC* mutant could potentially be explained by the activation of YAP in these animals, the increase of *Taz* mRNA levels in the β-*catenin*$^{\Delta ex3}$ jejunum suggests that TAZ must also be regulated transcriptionally through β-catenin. This effect is specific to *Taz*, as *Yap* mRNA levels were largely unaltered in either mutant background (Fig. 6E).

Since APC is a dual regulator of YAP and β-catenin and since TAZ is in turn regulated by both nuclear effectors, we wished to examine the functional contribution of TAZ to intestinal tumorigenesis upon loss of APC. We therefore examined whether inactivation of TAZ could suppress adenoma formation in the *APC*^{Min}/+ mice. Although TAZ is dispensable in normal intestinal homeostasis (Fig. 6C), inactivation of TAZ in the *APC*^{Min}/+ model (*VilCre;APC*^{Min}/+;*Taz*$^{flox/flox}$) nearly completely abolished adenoma formation in the small intestines (Fig. 6F). Real-time PCR revealed that the remaining adenomas in these animals were due to escaper cells that failed to delete *Taz* (Fig. 6G). We did not detect significant suppression of adenoma number in the colon (Fig. 6F). This is likely due to incomplete deletion of *Taz* in the colon, since the adenomas in the double-mutant colon still expressed high levels of *Taz* (Fig. 6G). These results suggest that, similar to YAP, TAZ is indispensable for intestinal tumorigenesis upon loss of APC.

Discussion

YAP is a critical downstream effector of APC independent of β-catenin

It is generally believed that β-catenin activation mediates intestinal tumorigenesis caused by APC mutations. The identification of stabilizing mutations of β-catenin in human colorectal cancers (Morin et al. 1997; Sparks et al. 1998) and the analysis of transgenic mice expressing stabilized β-catenin mutant protein (Harada et al. 1999; Romagnolo et al. 1999) provided further support for the role of activated β-catenin in *APC* mutant cancers. However, it has long been appreciated that human colorectal tumors with β-catenin-stabilizing mutations are less severe than those with APC mutations (Samowitz et al. 1999). In agreement with these observations, mice expressing stabilized β-catenin mutant protein exhibited a weaker intestinal phenotype compared with the *APC* mutant mice (Fig. 4A–C). This evidence suggests the existence of additional effectors besides β-catenin that mediate the tumor suppressor function of APC.

Our current study identifies YAP as one such effector (Fig. 7A). An important tenet of our model is that APC regulates Hippo–YAP signaling independently of its involvement in the β-catenin destruction complex. This model is supported by biochemical analysis revealing a direct role for APC in facilitating the Hippo kinase cascade (Fig. 3) as well as genetic analysis showing distinct YAP activation status in intestinal epithelia with APC inactivation versus those expressing a stabilized activated mutant of β-catenin (Fig. 2). In further support of this model, combined activation of YAP and β-catenin resulted in stronger intestinal phenotypes that more closely resemble those of APC deficiency (Fig. 4), and treatment of HEK293 cells with Wnt3a resulted in increased β-catenin levels without corresponding changes in YAP phosphorylation or activity (Supplemental Figs. S3F, S4). These results provide multiple lines of evidence supporting a novel function of APC in regulating YAP activity, separate from its well-established role in the β-catenin destruction complex. In agreement with our findings, Guan and colleagues (Park et al. 2015; K.-l. Guan, pers. comm.) found that Wnt3a did not affect YAP phosphorylation or protein levels in HEK293 cells but stimulated YAP/TAZ activity in other cell lines by noncanonical Wnt signaling independently of the destruction complex.

It remains to be determined how combined activation of YAP and β-catenin results in stronger intestinal phenotypes that more closely resemble APC deficiency (Fig. 4). A recent study suggested that cytoplasmic YAP suppressed Wnt–β-catenin signaling by restraining disheveled in the cytoplasm during intestinal regeneration (Barry et al. 2013). In our study, inactivation of APC, the dual regulator of YAP and β-catenin, represents a different context, in which both YAP and β-catenin accumulate in the nucleus and actively transcribe their target genes through association with the transcription factors TEAD and TCF/LEF, respectively. Besides engaging distinct transcription complexes, YAP and β-catenin have also been reported to associate with each other directly in a β-catenin–YAP1–TBX5 complex that is essential for the transformation and survival of β-catenin-driven cancers (Rosenbluh et al. 2012). This transcription complex can potentially contribute to the synergistic phenotype observed in animals with combined activation of YAP and β-catenin (Fig. 4) as well as the suppression of *APC*-deficient tumors by loss of YAP (Fig. 5). Besides genes regulated by YAP and/or β-catenin, our expression profiling suggests that APC also regulates additional targets independently of both YAP and β-catenin (Fig. 4D). Whether these non-YAP/β-catenin targets contribute to intestinal tumorigenesis upon APC inactivation requires further investigation.

Transcriptional regulation of TAZ by YAP and β-catenin

Similar to YAP, TAZ is regulated by Hippo signaling through a phosphorylation-dependent mechanism. Our

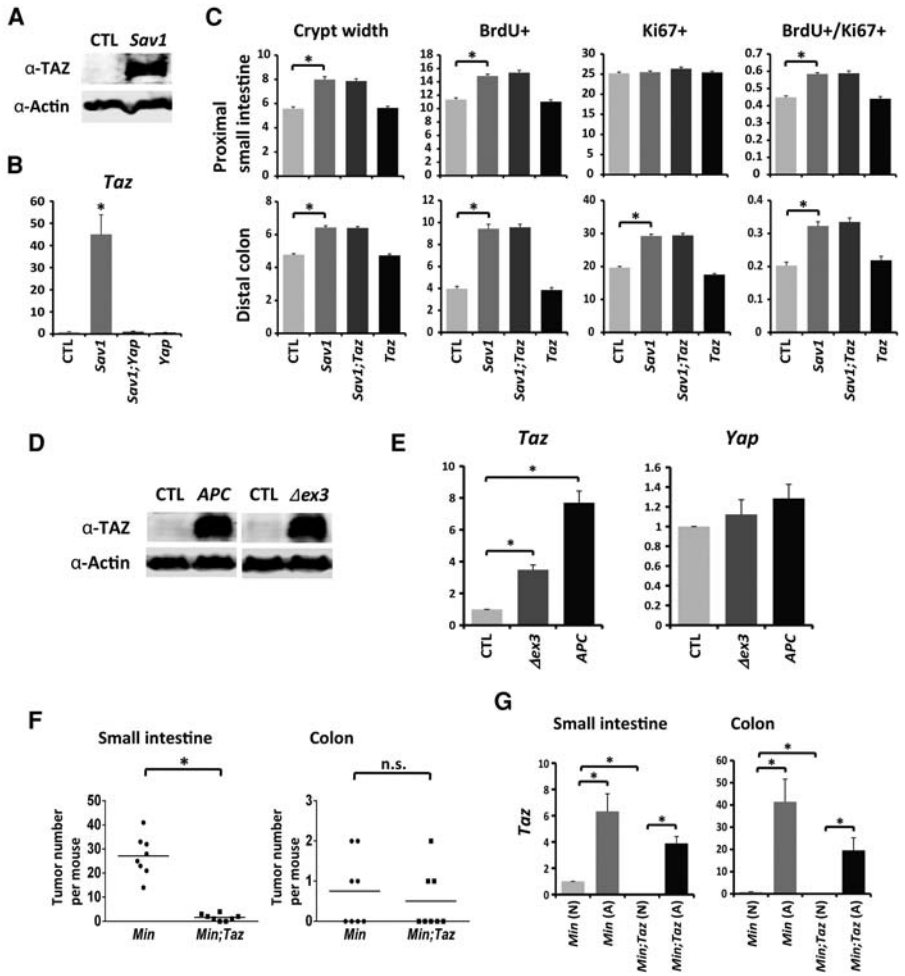

Figure 6. TAZ is transcriptionally regulated by YAP and β-catenin and is functionally required for intestinal tumorigenesis upon loss of APC. (*A*) Western blot analysis of TAZ in colonic crypts of 1-mo-old control and *Sav1*-deficient (*VilCre;Sav1*$^{flox/flox}$) mice. (*B*) Real-time PCR analysis of *Taz* mRNA levels in crypts of 1-mo-old control, *Sav1* mutant, *Yap* mutant (*VilCre;Yap*$^{flox/flox}$), and *Sav1;Yap* double-mutant (*VilCre;Sav1*$^{flox/flox}$*;Yap*$^{flox/flox}$) distal colons. Data are mean ± SD. $n = 3$. (*) $P < 0.005$, *t*-test. (*C*) Quantification of crypt width (3 mo old) and proliferation (1 mo old) in control, *Sav1* mutant (*VilCre;Sav1*$^{flox/flox}$), *Taz* mutant (*VilCre;Taz*$^{flox/flox}$), and *Sav1;Taz* double-mutant (*VilCre;Sav1*$^{flox/flox}$*;Taz*$^{flox/flox}$) proximal small intestines and distal colons. Data are mean ± SEM. (*) $P < 0.005$, *t*-test. (*D*) Western blot analysis of TAZ in control, *APC* mutant (*Lgr5-EGFP-IRES-creER*^{T2}*;APC*$^{flox/flox}$), and β-*catenin*$^{\Delta ex3}$ (*Lgr5-EGFP-IRES-creER*^{T2}*; Catnb*$^{+/lox(ex3)}$) jejunal tissues 4 wk after tamoxifen injection. (*E*) Real-time PCR analysis of *Taz* and *Yap* mRNA levels in control, β-*catenin*$^{\Delta ex3}$ (*Lgr5-EGFP-IRES-creER*^{T2}*;Catnb*$^{+/lox(ex3)}$), and *APC* mutant (*Lgr5-EGFP-IRES-creER*^{T2}*;APC*$^{flox/flox}$) jejunum 4 wk after tamoxifen injection. Data are mean ± SD. $n = 3$. (*) $P < 0.005$, *t*-test. (*F*) Quantification of the number of adenomas in the small intestines and colons of eight *APC*^{Min}/+;*Taz*$^{flox/flox}$ (*Min*) and eight *VilCre;APC*^{Min}/+;*Taz*$^{flox/flox}$ (*Min;Taz*) mice at the age of 3 mo. (*) $P < 0.005$; (n.s.) not significant, *t*-test. (*G*) Real-time PCR analysis of *Taz* mRNA levels in normal tissues (N) and adenomas (A) from the small intestines and the colons of *APC*^{Min}/+;*Taz*$^{flox/flox}$ (*Min*) and *VilCre;APC*^{Min}/+;*Taz*$^{flox/flox}$ (*Min;Taz*) mice. The *Taz* mRNA level was dramatically decreased in normal *VilCre;APC*^{Min}/+;*Taz*$^{flox/flox}$ (*Min;Taz*) tissue (0.133 ± 0.031) compared with normal *APC*^{Min}/+;*Taz*$^{flox/flox}$ (*Min*) tissue (set as 1). Both *APC*^{Min}/+;*Taz*$^{flox/flox}$ (*Min*) and *VilCre;APC*^{Min}/+;*Taz*$^{flox/flox}$ (*Min;Taz*) adenomas expressed high levels of *Taz* mRNA. Data are mean ± SD. $n = 3$. (*) $P < 0.005$, *t*-test.

current study uncovers a previously unappreciated role for YAP and β-catenin in regulating TAZ at the transcriptional level. Thus, APC may regulate TAZ activity through multiple mechanisms: phosphorylation of TAZ by the Hippo kinase cascade, transcriptional regulation through YAP, and transcriptional regulation through β-catenin. The transcriptional regulation of TAZ by YAP and β-catenin suggests that YAP and TAZ do not simply function redundantly in the intestine but also exhibit an additional epistatic relationship, with TAZ acting downstream from YAP (Fig. 7B). Our genetic analysis demonstrating that loss of either YAP or TAZ alone is sufficient to suppress the development of *APC*-deficient intestinal adenomas is consistent with such a relationship. We note that our findings that loss of YAP or TAZ alone is sufficient to suppress adenoma formation in *APC*^{min}/+ and *VilCre; APC*^{flox}/+ animals differ from a recent study (Azzolin et al. 2014) that concluded that combined inactivation

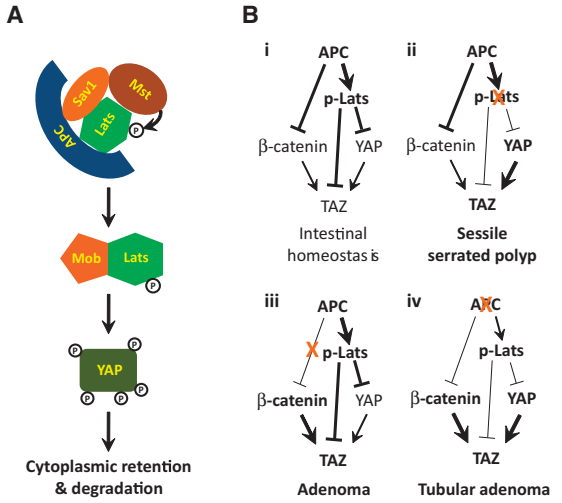

Figure 7. A schematic model showing APC-dependent regulation of Hippo–YAP signaling (*A*) and the contribution of YAP, β-catenin, and TAZ to intestinal tumorigenesis in various genetic backgrounds (*B*). (*A*) APC physically interacts with Sav1 and Lats and facilitates phosphorylation of Lats1/2 by Mst1/2. Activated Lats1/2 in complex with Mob1 phosphorylates YAP, resulting in its cytoplasmic retention and β-Trcp-mediated degradation. (*B*) Dual regulation of Hippo and Wnt signaling by APC. The transcriptional regulation of TAZ by YAP and β-catenin is also illustrated. (Panel *i*) Under physiological conditions, APC suppresses both YAP/TAZ and β-catenin to achieve intestinal homeostasis. (Panel *ii*) When Hippo signaling is perturbed (e.g., loss of Sav1), activation of YAP leads to development of SSPs in the colon, while APC retains its function to inactivate β-catenin. When β-catenin is stabilized through mutations that abolish its phosphorylation by GSK-3β and CK1, APC can still suppress YAP/TAZ activity through Hippo signaling. (Panel *iii*) Activation of β-catenin alone leads to adenoma development in the intestine. (Panel *iv*) Upon inactivation of APC, both YAP/TAZ and β-catenin are activated, resulting in the development of tubular adenomas.

of YAP and TAZ is required to suppress intestinal hyperplasia caused by acute loss of APC in a *VilCreER* model. Whether these differences are due to the different onset of APC loss (spontaneous loss during development vs. acute loss in adulthood) or YAP/TAZ loss (embryonic vs. adult deletion) remains to be determined.

The identification of APC as a dual regulator of Wnt–β-catenin and Hippo–YAP pathways has important implications for understanding its tumor suppressor function. We suggest that the characteristic tubular adenoma resulting from loss of APC is due to coactivation of β-catenin and YAP, whereas the activation of each oncoprotein alone results in less severe outcomes (Fig. 7B). Interestingly, unlike β-catenin, which is required for cell survival in intestinal epithelia (Ireland et al. 2004), YAP and TAZ are dispensable for normal intestinal homeostasis (Cai et al. 2010; Zhou et al. 2011; Azzolin et al. 2014). Our genetic analysis demonstrating that YAP or TAZ is absolutely required for intestinal tumorigenesis following APC inactivation therefore suggests that targeting YAP or TAZ may provide a more selective means against the *APC* mutant colorectal cancers with minimal effect on normal intestinal physiology compared with current approaches aimed at β-catenin inhibition (Lesko et al. 2014).

Materials and methods

Mouse genetics

APC^{Min}/+ (Moser et al. 1990; Su et al. 1992), *Villin-Cre* (Madison et al. 2002), $Catnb^{flox}$ (Brault et al. 2001), and *Rosa26-LacZ* mice (Soriano 1999) were from the Jackson Laboratory. $Catnb^{lox(ex3)}$ mice were described previously (Harada et al. 1999). *Lgr5-EGFP-IRES-creER*^{T2} mice (Barker et al. 2007) were kindly provided by Dr. Hans Clevers. APC^{flox} ($APC^{\Delta 14}$) mice (Colnot et al. 2004) were kindly provided by Dr. Christine Perret. Taz^{flox} mice (Xin et al. 2013) were kindly provided by Dr. Eric N. Olson.

Yap^{flox} (Zhang et al. 2010) and $Sav1^{flox}$ (Cai et al. 2010) mice were described previously. Mice with *Yap*, *Sav1*, *Taz*, or β-*catenin* specifically deleted in the intestinal epithelium were generated by breeding Yap^{flox}, $Sav1^{flox}$, Taz^{flox}, or $Catnb^{flox}$ mice with *Vil-Cre* mice. Mice with *APC* or *Sav1* inactivation or stabilized β-*catenin* specifically in the intestinal stem cells were generated by breeding APC^{flox}, $Sav1^{flox}$, or $Catnb^{lox(ex3)}$ mice with *Lgr5-EGFP-IRES-creER*^{T2} mice. Five daily intraperitoneal injections of 100 mg/kg tamoxifen (Sigma) dissolved in corn oil were performed in mice at 6 wk of age. Animal protocols were approved by the Institutional Animal Care and Use Committee of the Johns Hopkins University.

Cell culture analysis

ON-TARGETplus human APC, Lats1, and Lats2 siRNAs were from Thermo Scientific. BIO and XAV939 were from Sigma-Aldrich. Recombinant human Wnt3a was from R&D Systems. BIO and XAV939 were used at 10 µM. Wnt3a was used at 100 or 250 ng/mL. Transfection reagents Lipofectamine RNAi-MAX and Lipofectamine 2000 were from Life Technologies, and Effectene was from Qiagen.

Myc-Lats1-expressing, Myc-Sav1-expressing, HA-YAP-expressing, and HA-TEAD2-expressing vectors were described before (Dong et al. 2007; Liu-Chittenden et al. 2012). Flag-β-Trcp-expressing (#10865) (Zhou et al. 2000), HA-Sav1-expressing (#32834), HA-Mst2-expressing (#33098), HA-Mob1-expressing (#32835) (Zhao et al. 2007), and Flag-β-cateninS33Y-expressing (#19286) (Kolligs et al. 1999) vectors and TOP-FLASH (#12456) (Veeman et al. 2003) and 8xGTIIC-Lux (#34615) (Dupont et al. 2011) reporter plasmids were from Addgene. The Flag-tagged APC construct was amplified from expressing vector containing human full-length *APC* cDNA (Addgene # 16507) (Morin et al. 1997) with forward primer 5′-CCGGGATCCATGGATTACAAGGATGACGACGATAAGGCTGCAGCTTCATATGATCAG-3′ and reverse primer 5′-CCGGGATCCTTAAACAGATGTCACAAGGTAAGACCC-3′, subcloned into pGEM-T Easy vector, and confirmed by sequencing. The Flag-APC construct was released from pGEM-T Easy vector by BamHI digestion and subcloned into pCNDA3.1^{+} vector predigested with BamHI.

HEK293 cells were cultured in DMEM (Gibco-Life Technologies) supplemented with 10% FBS, L-glutamine, and antibiotics. *APC* knockout HEK293 cells were generated as described (Ran et al. 2013). Briefly, the guide oligos 5′-CACCGTGTATATCCATGCGACAGTC-3′and 5′-AAACGACTGTCGCATGGATATACAG-3′ were annealed and subcloned into pSpCas9(BB)-2A-Puro vector before transfection into HEK293 cells. Puromycin (1 µg/mL) was used for selection after transfection. Surviving cells were diluted in DMEM at a concentration of 0.5 cells per 100 µL and plated in 96-well plates. Colonies derived from single cells

were expanded, and APC mutant colonies were confirmed by Western blot and genome sequencing.

Immunofluorescence staining was performed according to the manufacturer's protocol of the antibodies. For luciferase assay, HEK293 cells were transfected with plasmids and washed with fresh medium the second day. Analysis was performed 24 h after the wash.

Mouse histological analysis and immunohistochemistry

Mouse intestinal samples were collected, fixed overnight in 4% paraformaldehyde in PBS, embedded in paraffin, and sectioned at 5 µm. Sections were stained with hematoxylin–eosin for histological analysis. Immunohistochemistry on serial sections was performed according to the manufacturers' protocols. Intraperitoneal injection of 30 mg/kg BrdU (Sigma) dissolved in 3 mg/mL 1× PBS was performed 2 h before tissue harvest. The primary antibodies used for immunohistochemistry were rabbit anti-β-catenin (1:500; Sigma), anti-YAP (1:100; Cell Signaling), anti-p-YAP (S127; 1:100; Cell Signaling), anti-YAP/TAZ (1:100; Cell Signaling), anti-Ki67 (1:1000; Novocastra), anti-Lats1 (1:100; Cell Signaling), and mouse anti-BrdU (1:50; Developmental Studies Hybridoma Bank). The signals were developed using the ABC kit purchased from Vector Laboratories according to the manufacturer's suggestions. Cy3-conjugated goat anti-rabbit and Alexa 488-conjugated goat anti-mouse secondary antibodies (Molecular Probes) were used for immunofluorescence.

Isolation of colonic crypts

Colons at ~1 cm away from the anus were cut longitudinally and rinsed in PBS to remove feces. Two-millimeter to 3-mm pieces of colons were incubated in PBS with 5 mM EDTA for 15 min at 37°C. Vigorous shaking released crypts. Crypts were photographed, and the width was measured in AxioVision release 4.7. For RNA and protein analysis, the supernatant containing free crypts was collected and centrifuged. The pellet was washed in ice-cold PBS and subjected to RNA extraction or snap-frozen in liquid nitrogen for Western blot analysis.

Microarray analysis

Jejunal tissues from control, *Sav1* mutant (*Lgr5-EGFP-IRES-creER^{T2};Sav1$^{flox/flox}$*), β-catenin-stabilized mutant [*Lgr5-EGFP-IRES-creER^{T2};Catnb$^{+/lox(ex3)}$*], β-catenin-stabilized/*Sav1* double-mutant [*Lgr5-EGFP-IRES-creER^{T2};Catnb$^{+/lox(ex3)}$;Sav1$^{flox/flox}$*], and *APC* mutant (*Lgr5-EGFP-IRES-creER^{T2};APC$^{flox/flox}$*) mice were harvested 4 wk after tamoxifen injection for total RNA extraction. Total RNA from each sample was quantified using the NanoDrop ND-1000, and RNA integrity was assessed by standard denaturing agarose gel electrophoresis. For microarray analysis, Agilent array platform was employed. The sample preparation and microarray hybridization were performed based on the manufacturer's standard protocols. Briefly, total RNA from each sample was amplified and transcribed into fluorescent cRNA using Agilent's quick amp labeling protocol (version 5.7, Agilent Technologies). The labeled cRNAs were hybridized onto the whole-mouse genome oligo microarray (Agilent Technologies, 4x44K). After the slides were washed, the arrays were scanned by the Agilent scanner G2505C. Agilent Feature Extraction software (version 11.0.1.1) was used to analyze the acquired array images. Quantile normalization and subsequent data processing were performed using GeneSpring GX version 11.5.1 software (Agilent Technologies). After quantile normalization of the raw data, genes that had at least three out of six samples with flags in Detected ("all targets value") were chosen for further data analysis. Differentially expressed genes with statistical significance were identified through Volcano Plot filtering. The default threshold was fold change of ≥2.0 (P-value ≤ 0.05). Pathway analysis was applied to determine the roles that these differentially expressed genes played in these biological pathways. Finally, hierarchical clustering was performed to show the distinguishable gene expression profiling among samples. Hybridization and raw data analysis were done by Arraystar, Inc.

Analysis of YAP and β-catenin status in human cancers

Formalin-fixed, paraffin-embedded sections were obtained from archival human tubular adenomas, pancreatic acinar cell carcinomas, ovarian serous carcinomas, and pancreatic ductal adenocarcinomas that had been surgically removed at the Johns Hopkins Hospital. The diagnosis of these cancers was rendered based on established criteria by specialized pathologists (A. Maitra and R. A. Anders). Heat-induced antigen retrieval was performed in a steamer using citrate buffer (pH 6.0; Vector Laboratories) for 25 min followed by 30 min of cooling. Nonspecific binding was blocked for 30 min with 5% goat serum in TBST. Serial sections were then incubated with two primary antibodies—anti-YAP (1:150; Epitomics) and anti-β-catenin (1:500; Sigma)—overnight at 4°C. The signals were developed using the ABC kit purchased from Vector Laboratories according to the manufacturer's suggestions. Finally, sections were counterstained with Harris hematoxylin, subsequently rehydrated in distilled H_2O and graded series of ethanol (70%, 95%, and 100%), and mounted.

Western blotting

Jejunal tissues and cultured cells were lysed, and the extracted proteins were analyzed. The primary antibodies used for Western blot were rabbit anti-Mst1 (1:1000; Cell Signaling), anti-p-Mst (1:1000; Cell Signaling), anti-Lats1 (1:1000; Cell Signaling), anti-p-Lats (Yu et al. 2010), anti-YAP (1:1000 [Cell Signaling, #4912], 1:1000 [Santa Cruz Biotechnology, H-9 and 63.7], and 1:1000 [Novus, NB110-58358]), anti-p-YAP (S127; 1:1000; Cell Signaling), anti-p-YAP (S381; 1:1000; Cell Signaling) (Kim et al. 2013), anti-β-catenin (1:2500; Sigma), anti-YAP/TAZ (1:1000; Cell Signaling), anti-Axin2 (1:1000; Cell Signaling), mouse anti-APC (1:200; Calbiochem, Ab-1), anti-Flag (1:5000; Sigma, M2), anti-HA (1:5000; Sigma), anti-Myc (1:2000; Calbiochem), anti-Actin (1:5000; Millipore), and rat anti-Flag (1:2000; BioLegend, L5). Signals were quantified by ImageJ.

Quantitative real-time PCR

RNAs from intestines was extracted using the TRIzol reagent (Invitrogen). RNA was reverse-transcribed using the iScrip cDNA synthesis kit (Bio-Rad). Quantitative real-time PCR was performed using the iQ SYBR Green supermix (Bio-Rad) on a CFX96 real-time system (Bio-Rad). The primers used for real-time PCR were as follows: *Yap*, 5′-TACATAAACCATAAGAACAAGACCACA-3′ (forward) and 5′-GCTTCACTGGAGCACTCTGA-3′ (reverse); *Taz*, 5′-GAAGGTGATGAATCAGCCTCTG-3′ (forward) and 5′-GTTCTGAGTCGGGTGGTTCTG-3′ (reverse); and *Gapdh*, 5′-CCCAATGTGTCCGTCGTGGAT-3′ (forward) and 5′-TGTAGCCCAAGATGCCCTTCAG-3′ (reverse).

Acknowledgments

We thank Dr. Hans Clevers for the kind gift of *Lgr5-EGFP-IRES-creER^{T2}* mice, Dr. Christine Perret for the kind gift of *APC^{flox}*

($APC^{\Delta 14}$) mice, Dr. Eric N. Olson for the kind gift of Taz^{flox} mice, and Dr. Dae-Sik Lim for the kind gift of anti-p-YAP (S381) antibody. This study was supported in part by grants from the Crohn's and Colitis Foundation of America (CCFA3582) and Maryland Stem Cell Research Fund (MSCRFF-0059). D.P. is an investigator of the Howard Hughes Medical Institute.

References

Abraham SC, Wu T-T, Hruban RH, Lee J-H, Yeo CJ, Conlon K, Brennan M, Cameron JL, Klimstra DS. 2002. Genetic and immunohistochemical analysis of pancreatic acinar cell carcinoma: frequent allelic loss on chromosome 11p and alterations in the APC/β-catenin pathway. *Am J Pathol* **160:** 953–962.

Aoki K, Taketo MM. 2007. Adenomatous polyposis coli (APC): a multi-functional tumor suppressor gene. *J Cell Sci* **120:** 3327–3335.

Azzolin L, Zanconato F, Bresolin S, Forcato M, Basso G, Bicciato S, Cordenonsi M, Piccolo S. 2012. Role of TAZ as mediator of Wnt signaling. *Cell* **151:** 1443–1456.

Azzolin L, Panciera T, Soligo S, Enzo E, Bicciato S, Dupont S, Bresolin S, Frasson C, Basso G, Guzzardo V. 2014. YAP/TAZ incorporation in the β-catenin destruction complex orchestrates the Wnt response. *Cell* **158:** 157–170.

Barker N, van Es JH, Kuipers J, Kujala P, van den Born M, Cozijnsen M, Haegebarth A, Korving J, Begthel H, Peters PJ. 2007. Identification of stem cells in small intestine and colon by marker gene Lgr5. *Nature* **449:** 1003–1007.

Barker N, Ridgway RA, van Es JH, van de Wetering M, Begthel H, van den Born M, Danenberg E, Clarke AR, Sansom OJ, Clevers H. 2009. Crypt stem cells as the cells-of-origin of intestinal cancer. *Nature* **457:** 608–611.

Barry ER, Morikawa T, Butler BL, Shrestha K, de La Rosa R, Yan KS, Fuchs CS, Magness ST, Smits R, Ogino S. 2013. Restriction of intestinal stem cell expansion and the regenerative response by YAP. *Nature* **493:** 106–110.

Brault V, Moore R, Kutsch S, Ishibashi M, Rowitch DH, McMahon AP, Sommer L, Boussadia O, Kemler R. 2001. Inactivation of the β-catenin gene by Wnt1-Cre-mediated deletion results in dramatic brain malformation and failure of craniofacial development. *Development* **128:** 1253–1264.

Cai J, Zhang N, Zheng Y, de Wilde RF, Maitra A, Pan D. 2010. The Hippo signaling pathway restricts the oncogenic potential of an intestinal regeneration program. *Genes Dev* **24:** 2383–2388.

Colnot S, Niwa-Kawakita M, Hamard G, Godard C, Le Plenier S, Houbron C, Romagnolo B, Berrebi D, Giovannini M, Perret C. 2004. Colorectal cancers in a new mouse model of familial adenomatous polyposis: influence of genetic and environmental modifiers. *Lab Invest* **84:** 1619–1630.

Couzens AL, Knight JD, Kean MJ, Teo G, Weiss A, Dunham WH, Lin Z-Y, Bagshaw RD, Sicheri F, Pawson T. 2013. Protein interaction network of the mammalian Hippo pathway reveals mechanisms of kinase-phosphatase interactions. *Sci Signal* **6:** rs15–rs15.

Dong J, Feldmann G, Huang J, Wu S, Zhang N, Comerford SA, Gayyed MF, Anders RA, Maitra A, Pan D. 2007. Elucidation of a universal size-control mechanism in *Drosophila* and mammals. *Cell* **130:** 1120–1133.

Dupont S, Morsut L, Aragona M, Enzo E, Giulitti S, Cordenonsi M, Zanconato F, Le Digabel J, Forcato M, Bicciato S. 2011. Role of YAP/TAZ in mechanotransduction. *Nature* **474:** 179–183.

Gregorieff A, Clevers H. 2005. Wnt signaling in the intestinal epithelium: from endoderm to cancer. *Genes Dev* **19:** 877–890.

Halder G, Johnson RL. 2011. Hippo signaling: growth control and beyond. *Development* **138:** 9–22.

Harada N, Tamai Y, Ishikawa To, Sauer B, Takaku K, Oshima M, Taketo MM. 1999. Intestinal polyposis in mice with a dominant stable mutation of the β-catenin gene. *EMBO J* **18:** 5931–5942.

Ireland H, Kemp R, Houghton C, Howard L, Clarke AR, Sansom OJ, Winton DJ. 2004. Inducible Cre-mediated control of gene expression in the murine gastrointestinal tract: effect of loss of β-catenin. *Gastroenterology* **126:** 1236–1246.

Kim M, Kim M, Lee S, Kuninaka S, Saya H, Lee H, Lee S, Lim DS. 2013. cAMP/PKA signalling reinforces the LATS–YAP pathway to fully suppress YAP in response to actin cytoskeletal changes. *EMBO J* **32:** 1543–1555.

Kolligs FT, Hu G, Dang CV, Fearon ER. 1999. Neoplastic transformation of RK3E by mutant β-catenin requires deregulation of Tcf/Lef transcription but not activation of *c-myc* expression. *Mol Cell Biol* **19:** 5696–5706.

Konsavage WM, Kyler SL, Rennoll SA, Jin G, Yochum GS. 2012. Wnt/β-catenin signaling regulates Yes-associated protein (YAP) gene expression in colorectal carcinoma cells. *J Biol Chem* **287:** 11730–11739.

Kwon Y, Vinayagam A, Sun X, Dephoure N, Gygi SP, Hong P, Perrimon N. 2013. The Hippo signaling pathway interactome. *Science* **342:** 737–740.

Lesko AC, Goss KH, Prosperi JR. 2014. Exploiting APC function as a novel cancer therapy. *Curr Drug Targets* **15:** 90–102.

Liu-Chittenden Y, Huang B, Shim JS, Chen Q, Lee S-J, Anders RA, Liu JO, Pan D. 2012. Genetic and pharmacological disruption of the TEAD–YAP complex suppresses the oncogenic activity of YAP. *Genes Dev* **26:** 1300–1305.

Madison BB, Dunbar L, Qiao XT, Braunstein K, Braunstein E, Gumucio DL. 2002. Cis elements of the villin gene control expression in restricted domains of the vertical (crypt) and horizontal (duodenum, cecum) axes of the intestine. *J Biol Chem* **277:** 33275–33283.

Markowitz SD, Bertagnolli MM. 2009. Molecular basis of colorectal cancer. *N Engl J Med* **361:** 2449–2460.

Morin PJ, Sparks AB, Korinek V, Barker N, Clevers H, Vogelstein B, Kinzler KW. 1997. Activation of β-catenin–Tcf signaling in colon cancer by mutations in β-catenin or APC. *Science* **275:** 1787–1790.

Moser AR, Pitot HC, Dove WF. 1990. A dominant mutation that predisposes to multiple intestinal neoplasia in the mouse. *Science* **247:** 322–324.

Näthke I. 2006. Cytoskeleton out of the cupboard: colon cancer and cytoskeletal changes induced by loss of APC. *Nat Rev Cancer* **6:** 967–974.

Pan D. 2010. The hippo signaling pathway in development and cancer. *Dev Cell* **19:** 491–505.

Park HW, Kim YC, Yu B, Moroishi T, Mo J-S, Plouffe SW, Meng Z, Lin KC, Yu F-X, Alexander CM, et al. 2015. Alternative Wnt signaling activates YAP/TAZ. *Cell* (in press).

Ran FA, Hsu PD, Wright J, Agarwala V, Scott DA, Zhang F. 2013. Genome engineering using the CRISPR–Cas9 system. *Nat Protoc* **8:** 2281–2308.

Rex DK, Ahnen DJ, Baron JA, Batts KP, Burke CA, Burt RW, Goldblum JR, Guillem JG, Kahi CJ, Kalady MF. 2012. Serrated lesions of the colorectum: review and recommendations from an expert panel. *Am J Gastroenterol* **107:** 1315–1329.

Romagnolo B, Berrebi D, Saadi-Keddoucci S, Porteu A, Pichard A-l, Peuchmaur M, Vandewalle A, Kahn A, Perret C. 1999.

Intestinal dysplasia and adenoma in transgenic mice after overexpression of an activated β-catenin. *Cancer Res* **59:** 3875–3879.

Rosenbluh J, Nijhawan D, Cox AG, Li X, Neal JT, Schafer EJ, Zack TI, Wang X, Tsherniak A, Schinzel AC. 2012. β-Catenin-driven cancers require a YAP1 transcriptional complex for survival and tumorigenesis. *Cell* **151:** 1457–1473.

Samowitz WS, Powers MD, Spirio LN, Nollet F, Van Roy F, Slattery ML. 1999. β-Catenin mutations are more frequent in small colorectal adenomas than in larger adenomas and invasive carcinomas. *Cancer Res* **59:** 1442–1444.

Soriano P. 1999. Generalized lacZ expression with the ROSA26 Cre reporter strain. *Nat Genet* **21:** 70–71.

Sparks AB, Morin PJ, Vogelstein B, Kinzler KW. 1998. Mutational analysis of the APC/β-catenin/Tcf pathway in colorectal cancer. *Cancer Res* **58:** 1130–1134.

Steinhardt AA, Gayyed MF, Klein AP, Dong J, Maitra A, Pan D, Montgomery EA, Anders RA. 2008. Expression of Yes-associated protein in common solid tumors. *Hum Pathol* **39:** 1582–1589.

Su L-K, Kinzler KW, Vogelstein B, Preisinger AC, Moser AR, Luongo C, Gould KA, Dove WF. 1992. Multiple intestinal neoplasia caused by a mutation in the murine homolog of the APC gene. *Science* **256:** 668–670.

Veeman MT, Slusarski DC, Kaykas A, Louie SH, Moon RT. 2003. Zebrafish prickle, a modulator of noncanonical Wnt/Fz signaling, regulates gastrulation movements. *Curr Biol* **13:** 680–685.

Wang J, Park J-S, Wei Y, Rajurkar M, Cotton JL, Fan Q, Lewis BC, Ji H, Mao J. 2013. TRIB2 acts downstream of Wnt/TCF in liver cancer cells to regulate YAP and C/EBPα function. *Mol Cell* **51:** 211–225.

Xin M, Kim Y, Sutherland LB, Murakami M, Qi X, McAnally J, Porrello ER, Mahmoud AI, Tan W, Shelton JM. 2013. Hippo pathway effector Yap promotes cardiac regeneration. *Proc Natl Acad Sci* **110:** 13839–13844.

Yu J, Zheng Y, Dong J, Klusza S, Deng W-M, Pan D. 2010. Kibra functions as a tumor suppressor protein that regulates Hippo signaling in conjunction with Merlin and Expanded. *Dev Cell* **18:** 288–299.

Zhang N, Bai H, David KK, Dong J, Zheng Y, Cai J, Giovannini M, Liu P, Anders RA, Pan D. 2010. The Merlin/NF2 tumor suppressor functions through the YAP oncoprotein to regulate tissue homeostasis in mammals. *Dev Cell* **19:** 27–38.

Zhao B, Wei X, Li W, Udan RS, Yang Q, Kim J, Xie J, Ikenoue T, Yu J, Li L. 2007. Inactivation of YAP oncoprotein by the Hippo pathway is involved in cell contact inhibition and tissue growth control. *Genes Dev* **21:** 2747–2761.

Zhao B, Li L, Lei Q, Guan K-L. 2010a. The Hippo–YAP pathway in organ size control and tumorigenesis: an updated version. *Genes Dev* **24:** 862–874.

Zhao B, Li L, Tumaneng K, Wang C-Y, Guan K-L. 2010b. A coordinated phosphorylation by Lats and CK1 regulates YAP stability through SCFβ–TRCP. *Genes Dev* **24:** 72–85.

Zhou P, Bogacki R, McReynolds L, Howley PM. 2000. Harnessing the ubiquitination machinery to target the degradation of specific cellular proteins. *Mol Cell* **6:** 751–756.

Zhou D, Zhang Y, Wu H, Barry E, Yin Y, Lawrence E, Dawson D, Willis JE, Markowitz SD, Camargo FD. 2011. Mst1 and Mst2 protein kinases restrain intestinal stem cell proliferation and colonic tumorigenesis by inhibition of Yes-associated protein (Yap) overabundance. *Proc Natl Acad Sci* **108:** E1312–E1320.